TEKTONIKA

Fingerprinting Fluid Source in Calcite Veins: Combining LA-ICP-MS U-Pb Calcite Dating with Trace Elements and Clumped Isotope Palaeothermometry

J. M. MacDonald *[1], **J. VanderWal**[2], **N. M. W. Roberts**[3], **I. Z. Winkelstern**[4], **J. W. Faithfull**[5], **A. J. Boyce**[6]

[1]School of Geographical and Earth Sciences, University of Glasgow, Glasgow G12 8QQ, UK | [2]Barrick Gold, Hwy 17, Marathon, ON, P0T 2E0, Canada | [3]Geochronology and Tracers Facility, British Geological Survey, Environmental Science Centre, Nottingham, NG12 5GG, UK | [4]Department of Geology, Grand Valley State University, Padnos Hall of Science, 1 Campus Drive, Allendale, MI 49401, USA | [5]The Hunterian, University of Glasgow, Glasgow G12 8QQ, UK | [6]NERC Isotope Community Support Facility, Scottish Universities Environmental Research Centre, Rankine Avenue, Scottish Enterprise Technology Park, East Kilbride G75 0QF, UK

Abstract Application of geochemical proxies to vein minerals - particularly calcite - can fingerprint the source of fluids controlling various important geological processes from seismicity to geothermal systems. Determining fluid source, e.g. meteoric, marine, magmatic or metamorphic waters, can be challenging when using only trace elements and stable isotopes as different fluids can have overlapping geochemical characteristics, such as $\delta^{18}O$. In this contribution we show that by combining the recently developed LA-ICP-MS U-Pb calcite geochronometer with stable isotopes (including clumped isotope palaeothermometry) and trace element analysis, the fluid source of veins can be more readily determined. Calcite veins hosted in the Devonian Montrose Volcanic Formation at Lunan Bay in the Midland Valley Terrane of Central Scotland were used as a case study. δD values of fluid inclusions in the calcite, and parent fluid $\delta^{18}O$ values reconstructed from clumped isotope palaeothermometry, gave values which could represent a range of fluid sources: metamorphic or magmatic fluids, or surface waters which had undergone much fluid-rock interaction. Trace elements showed no particularly distinctive patterns. LA-ICP-MS U-Pb dating determined the vein calcite precipitation age – 318±30 Ma – indicating a metamorphic or magmatic fluid source was unlikely as there was no metamorphic or magmatic activity was occurring in the area at this time. The vein fluid source was therefore interpreted to be a surface water (meteoric based on paleogeographic reconstruction) which had undergone significant water-rock interaction. This study highlights the importance of combining the recently developed LA-ICP-MS U-Pb calcite geochronometer with stable isotopes and trace elements to help determine fluid sources of veins, and indeed any geological feature where calcite precipitated from a fluid that may have resided in the crust for a period of time (e.g. fault precipitates or cements).

Executive Editor:
R. da Silva Schmitt
Technical Editor:
Mohamed Gouiza

Reviewers:
Everton Bongiolo
John Craddock

Submitted:
15 August 2022
Accepted:
27 November 2023
Published:
5 February 2024

1 Introduction

Fingerprinting the source of fluids flowing through fractures in the crust has importance in a range of geological applications, including: 1) understanding the origin, and predicting sustainability, of geothermal systems (e.g. *Simmons and Christenson*, 1994; *Menzies et al.*, 2014; *Lu et al.*, 2017, 2018); 2) determining the origin and concentration of economic mineral deposits (e.g. *Barker and Cox*, 2011; *Bongiolo et al.*, 2011); and 3) reconstructing fluid flow pathways responsible for seismicity (e.g. *Uysal et al.*, 2011; *Nuriel et al.*, 2017; *Sturrock et al.*, 2017; *Nuriel et al.*, 2019; *Weinberger et al.*, 2020; *Craddock et al.*, 2022). Evidence of palaeofluid flow through fractures is recorded by the presence of veins (*Ramsay and Huber*, 1983) and application of geochemical proxies to vein minerals - particularly calcite - can enable reconstruction of fluid sources.

If stable isotope signatures of vein-forming minerals can be reconstructed, then this has the potential to enable fluid source identification. The hydrogen isotopic signature (δD) of vein-forming fluids can be measured by decrepitation if there is a high enough volume of fluid inclusions within the vein-filling calcite (*Gleeson et al.*, 2008). Fluid $\delta^{18}O$ can be calculated by determining the calcite

*john.macdonald.3@glasgow.ac.uk

$\delta^{18}O$ and the temperature of precipitation (e.g. *Epstein et al.*, 1951). Precipitation temperature of calcite veins can be reconstructed from fluid inclusion microthermometry (e.g. *Barker and Goldstein*, 1990; *Maskenskaya et al.*, 2014) or the more recently-developed clumped isotope palaeothermometer. Clumped isotope palaeothermometry utilises the temperature dependence of different isotopologues of CO_2, particularly the mass 47 ^{13}C-^{18}O-^{16}O isotopologue (e.g. *Schauble et al.*, 2006; *Eiler*, 2007). Calcite vein precipitation temperatures have been reconstructed using clumped isotopes in geothermal/hydrothermal systems (*Lu et al.*, 2017, 2018; *MacDonald et al.*, 2019; *Swennen et al.*, 2021), sedimentary basins (e.g. *Mangenot et al.*, 2018a; *Pagel et al.*, 2018; *Staudigel et al.*, 2018; *Li et al.*, 2020; *Purvis et al.*, 2020) and fault systems (*Bergman et al.*, 2013; *Hodson et al.*, 2016; *Dennis et al.*, 2019; *Hoareau et al.*, 2021; *Looser et al.*, 2021; *Riegel et al.*, 2022).

Stable isotope analysis can therefore provide details of the vein-forming fluid source. Different fluids (e.g. magmatic, metamorphic, meteoric, seawater) have typical compositions inδD-$\delta^{18}O$ (V-SMOW) space (e.g. *Craig*, 1961; *Taylor*, 1974; *Rollinson*, 1993; *Sharp*, 2017; *Hoefs*, 2015). However, these different fluids may have overlapping compositions, or their isotopic composition may have changed over time. For example, a water withδD of -50‰ and $\delta^{18}O$ of +8‰ could be a magmatic water or a metamorphic water (e.g. *Hoefs*, 2015); equally though, it could be a meteoric water which has undergone significant water-rock equilibration resulting in an enrichment of $\delta^{18}O$ (e.g. *Menzies et al.*, 2014). Thus, fluid stable isotope signatures in themselves do not always provide a conclusive fingerprint of palaeofluid sources, especially in settings such as veins where there is scope for significant water-rock interaction, and where the genetic context of the hydrothermal system may be equivocal.

Previous studies attempting to determine the origin of vein-forming fluids have often analysed trace element concentrations in addition to stable isotopes. *Barker et al.* (2006) suggested varying trace element concentrations (and stable isotope values) in anti-taxial veins could be caused by cycles of fluid influx, water-rock interaction, and/or crack-seal processes. *Maskenskaya et al.* (2014) found that trace element concentrations and distribution in veins did not correlate with stable isotope (C, O, Sr) values; fractionation patterns of rare earth elements (REEs) were observed but again these could not be correlated with any measured chemical, physical and isotopic variables and so did not help to determine fluid source or vein formation mechanisms. *Kalliomäki et al.* (2019) compared the trace element signatures of calcite veins and their host rock and showed in examples from the Hattu schist belt (Finland) that interaction between the vein-forming fluid and the host rock had strongly influenced the trace element signature of the resulting calcite veins. Similarly, *Wagner et al.* (2010) used REEs to show that veins from the Rhenish Massif (Germany) formed from advecting fluids which leached the wall rocks, which was reflected in vein mineral trace element signatures. *Herlambang and John* (2021) paired trace element (Fe and Mn) concentrations with clumped isotope palaeothermometry in calcite veins from Jebel Madar, Oman, and found a strong correlation between trace element concentration and clumped isotope temperature. This indicated variable calcite crystal growth rates, causing potential kinetic fractionation in clumped isotopes.

The geological history of an area provides crucial context for discussion of potential fluid sources. In a metamorphic terrane, clearly metamorphic fluids may be recorded. With veins, however, fluid circulation may come sometime after formation of the surrounding geology and so linking vein-forming fluids to host rocks can be complex. Establishing the age of precipitation of veins is therefore key to understanding the geological context of vein formation, and thus the fluids involved. For example, if a vein with a calculated fluid $\delta^{18}O$ of +9‰ andδD of -50‰ can be dated to within error of formation of nearby basalts, then a contribution of magmatic fluids to vein precipitation cannot be excluded. The recent development of calcite U-Pb dating via Laser Ablation Inductively Coupled Mass Spectrometry (LA-ICP-MS) has enabled precise, accurate and rapid dating of calcite (e.g. *Li et al.*, 2014; *Coogan et al.*, 2016; *Ring and Gerdes*, 2016; *Roberts and Walker*, 2016; *Nuriel et al.*, 2017; *Roberts et al.*, 2017; *Drost et al.*, 2018). MacDonald et al., (2019) used this technique to date calcite veins from ancient hydrothermal systems to show that closed-system bond reordering (*Passey and Henkes*, 2012; *Henkes et al.*, 2014; *Stolper and Eiler*, 2015) – i.e. post-crystallisation diffusion of atoms in the calcite crystal lattice – did not affect determination of vein precipitation temperature from clumped isotopes. *Hoareau et al.* (2021) also combined clumped isotope palaeothermometry and calcite U-Pb LA-ICP-MS geochronology on calcite veins in the Pyrenees but modelled that the clumped isotopes in some of their older veins were reset by closed-system bond reordering.

In this contribution, we show that combining LA-ICP-MS U-Pb dating of calcite veins with stable isotope and trace element analyses can help to fingerprint fluid source when trace elements and fluidδD & $\delta^{18}O$ cannot always provide an unequivocal interpretation. We use a case study of volcanic-hosted veins in eastern Scotland, where this combination of proxies enables us to rule out magmatic fluids, indicating the fluid source of veins was meteoric water which had undergone significant water-rock interaction.

2 Geological Setting and Sample Petrography

Calcite veins from Lunan Bay in Angus (Figure 1a-b), Scotland formed the basis of this study. The study area is located within the northern part of the Midland Valley Terrane (e.g. *Trewin*, 2002). The host rocks to the calcite veins are the Montrose Volcanic Formation (MVF), a group of mingled pahoehoe lavas, basaltic andesites, and volcanic-derived sediments deposited as part of the ~2000 m thick, sandstone dominated Devonian age Arbuthnott-Garvock Group (e.g. *Armstrong and Paterson*, 1970; *Bluck*, 2000; *Browne et al.*, 2002; *Hole et al.*, 2013). These lavas are likely sourced from the northern flank of the Montrose Volcanic Centre, a north-east to south-west trending chain of volcanoes active for ~15 Myr. The MVF lavas are suggested to be coeval with the Rhynie lavas to the north, with a U-Pb zircon age of 411.5$\pm$1.3 Ma from andesite (*Parry et al.*, 2011). This places the MVF within the Devonian and at the boundary of the Arbuthnott and Garvock units (e.g. *Armstrong and Paterson*, 1970; *Bluck*, 2000; *Browne et al.*, 2002; *Hole et al.*, 2013).

The MVF lavas are basaltic to basaltic andesite (5.2-8.6 wt.% MgO, 52.6-57.6 wt.% SiO_2) in composition, and are olivine-plagioclase phyric, with olivine commonly pseudomorphed to iddingsite (*Thirlwall*, 1981, 1982, 1983). Sub-euhedral, tabular, microphenocrystic plagioclase feldspar (labradorite to andesine, An41-55) make up much of the matrix, along with abundant interstitial devitrified glass (*Thirlwall*, 1982). Clinopyroxene is also present within some of the pahoehoe lava flows, predominantly in the form of augite (*Hole et al.*, 2013). The lavas are also interbedded with locally sourced ephemeral playa-lake sediments, sandstones, and conglomerates, as well as air fall eruptions, creating complex sediment-lava interactions and abundant peperite formation (e.g. *Hole et al.*, 2013). Within these mixing regions, secondary orthoclase is also present. Sub-parallel flow alignment of feldspar laths and microphenocrysts is common (*Thirlwall*, 1982, 1983).

Samples of different MVF-hosted calcite veins were taken from the low cliffs just at the head of Lunan Bay at NO 69549 52488 (56°39'47.5"N, 02°29'54.1"W) (Figure 1c). Images of vein petrography and relations to geochemical analysis are provided in Supporting Information Figures SI-1 and SI-2. Most veins appear to be randomly oriented, with abundant stock work veining present; there is no clear field evidence of difference generations of veins. Five samples – JV17-1, -2, -9, -11 & -12 – were collected for analysis. The veins analysed in this study varied from >50 mm in width to less than 5 mm (Figure 1d-e). Primary vein formation is along a singular opening (JV17-1, JV17-2, JV17-9), although some veins also occur as a bundle of connected sub parallel veins (JV17-12). Within these veins, multiple forms of calcite growth were recognized including bladed (JV17-1) and toothy (JV17-2, JV17-9) calcites along host rock contacts (Figure SI-1, Supporting Information), while euhedral, scalenohedral, and blocky crystals making up the bulk of most vein matrices (JV17-1, JV17-2, JV17-12) (Figure SI-1, Supporting Information). Crosscutting relationships and alteration are readily observed in JV17-1a, where a primarily syntaxial, bedrock growth phase is crosscut by a secondary, anhedral growth phase, and in JV17-11, where a stretched vein is crosscut by an reddish calcite vein. Multiple phases are also evidenced by bedrock fragments and remnant calcite crystal growth along these fragments that have been sealed within the vein during subsequent vein sealing (JV17-1, JV17-12) (Figure SI-1, Supporting Information).

JV17-11 contains the only formation of stretched beef-veining (appearing similar to beef tendons), progressing from stretched/bladed crystals with vein opening (Figure SI-1, Supporting Information), although other samples not included within this study were also observed to have significant beef veining. Minor veins are prevalent in many of the samples (JV171, JV17-2, JV17-9, JV17-11), predominantly sealed with fine, euhedral calcite crystals only a few mm in size. Accessory minerals (quartz and chlorite) are visible along the vein-bedrock contacts, while reddish sutures are visible during the final stage of vein formation/closure in JV17-1 and JV17-2, consisting primarily of iron oxides and other rare carbonate phases (Figure SI-1, Supporting Information). These suture-defined vugs are filled with predominantly cloudy, anhedral calcites. Despite the variations in texture, only JV17-11 exhibits antitaxial vein growth (Figure SI-1, Supporting Information).

Minor variations in CL can be seen within the larger individual euhedral-anhedral blocky crystals that make up the bulk of the vein matrix in JV17-1 and JV17-2 (Figure SI-1, Supporting Information). However, CL signatures are generally uniform across individual veins and amygdales despite textural variation, with primary excitation associated with calcite cleavage planes and extinction (Figure SI-1, Supporting Information).

3 Methods

Cathodoluminescence (CL) petrography was undertaken using a Lumin HC4-LM hot-cathode CL microscope at Saint Marys University. Plane-polarized and CL imagery was taken using an incorporated Olympus BXFM focusing unit and Kappa DX40C peltier cooled camera, controlled by the DX40C-285FW software package. The samples were analyzed under a vacuum, with an accelerating voltage of ~6 KV, a beam current of 0.25 mA, and a 1 s camera exposure time with a 6 db camera gain.

$\delta^{13}C$ and $\delta^{18}O$ measurements were made at either the Scottish Universities Environmental Research Centre (SUERC) or Memorial University Newfoundland's TERRA Stable Isotope Lab. At

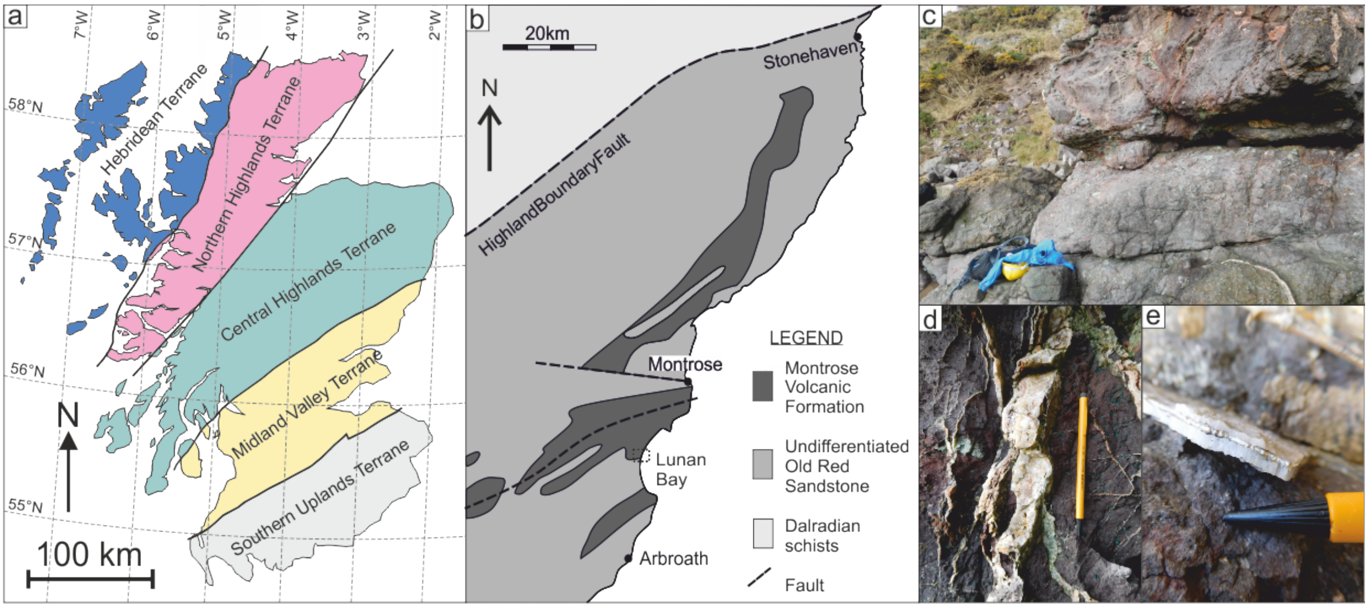

Figure 1 – Location and field photographs. **(a)** Location of Lunan Bay case study site within Scotland; **(b)** the distribution of the host Montrose Volcanic Formation in the region; **(c)** field photograph showing calcite veins in the host andesite (30 cm-diameter yellow hard hat for scale); Field photographs of examples veins **(d)** JV17-1 and **(e)** JV17-11.

Memorial, 0.2 mg of powdered sample was digested in 100% phosphoric acid in a 25°C water bath prior to analysis in a using a DeltaVPlus isotope ratio mass spectrometer (IRMS) equipped with a Thermo Electron GasBench II unit. NBS19, plus two internal standards, were used to calibrate the results, with NBS19 $\delta^{13}C$ of 2.0±0.1‰ and $\delta^{18}O$ of -2.2±0.1‰ (2σ), within error of accepted values (*Friedman et al.*, 1982; *Coplen et al.*, 2006) (Table SI-1, Supporting Data). At SUERC, 1 mg of powdered sample was digested in 100% phosphoric acid in a 25°C water bath prior to analysis in a VG OPTIMA mass spectrometer. Samples were run in triplicate and analytical uncertainties of 0.10‰ on $\delta^{13}C$ and 0.10‰ on $\delta^{18}O$ (2σ) were obtained on measurements of a marble standard (atc-1) measured during the analytical batch (n = 7) which are within error of the long term average (Table SI-1, Supporting Data).

δD values of entrapped water in fluid inclusions in calcite vein chips were measured by in vacuo decrepitation following the procedures outlined by *Gleeson et al.* (2008) at the Scottish Universities Environmental Research Centre (Table SI-2, Supporting Data). Procedural reproducibility was tested with 3 in-house standards (*Gleeson et al.*, 2008) and values were within 3‰ of long-term averages.

Carbonate clumped isotope (Δ_{47}) measurements were carried out in the Isotopologue Paleosciences Laboratory at the University of Michigan, Ann Arbor. Samples were powdered using a dental drill. For Δ_{47} analysis, ~8 mg of sample powder was reacted in an automated preparation line previously described in *Henkes et al.* (2014). Carbonate powder was reacted under vacuum with 104% phosphoric acid at 90°C for 10 min. Vapour-phase water generated during the reaction was separated from the produced CO_2 using liquid nitrogen swapped out an ethanol–liquid nitrogen mixture held at −85°C. The water remained frozen while the CO_2 was passed through a Poropak Q chromatography trap held at −20°C. The purified CO_2 was measured using a Nu Instruments Perspective isotope ratio mass spectrometer in dual inlet mode, with a measurement time of c. 2 hrs. All analyses were run as triplicates. Masses 44–49 were measured. Carrara marble, NBS19 and an in-house carbonate standard (102-GCAZ) were used to verify the results. Carrara Marble Δ_{47} averaged 0.417±0.022‰ (2σ, n=3), NBS19 Δ_{47} averaged 0.441±0.021‰ (2σ, n=10) and 102-GCAZ averaged 0.650±0.012‰ (2σ, n=14) during the analytical window. (Table SI-3, Supporting Data).

All carbonate clumped isotope (Δ_{47}) values in this study are presented on an absolute reference frame, also termed a 'carbon dioxide equilibrium scale' or CDES, which empirically corrects for instrumental nonlinearities and changes in the ionization environment during mass spectrometry (*Dennis et al.*, 2011; *Henkes et al.*, 2013). This reference frame was established by periodically analyzing aliquots of CO_2 that were isotopically equilibrated at 25 or 1000°C (*Dennis et al.*, 2011). Temperatures were calculated from Δ_{47} using the empirical "high temperature" Δ_{47} -temperature relationship from *Bonifacie et al.* (2017). Fluid $\delta^{18}O$ values were calculated using the equation of *Friedman* (1977).

Minor and trace element LA-ICP-MS analyses were undertaken at the Dalhousie Laboratory for Experimental High Pressure Geological Research using a New Wave Research frequency quintupled laser operating at 213 nm, coupled to a quadrupole mass spectrometer (PQ Excell or Thermo X-series) with He flushing. The analyses occurred as both linescans and spot analyses, with a 100µm spot size, ablated at 4-5 Hz with a 20% total energy. Concentrations of ^{43}Ca, ^{55}Mn, ^{57}Fe, ^{85}Rb, ^{86}Sr, ^{87}Sr, ^{89}Y, ^{137}Ba, ^{139}La, ^{140}Ce, ^{141}Pr, ^{146}Nd, ^{147}Sm, ^{153}Eu, ^{157}Gd, ^{159}Tb, ^{163}Dy, ^{165}Ho, ^{166}Er, ^{169}Tm, ^{172}Yb, and ^{175}Lu were measured in blocks of sixteen analyses, with two NIST 610 bounding each block for a total of 20 analyses per run. Total run times were 140 s, with 20 s laser warm-up, 60 s ablation, and 60 s He-gas flushing time. However, due to calcite burn through, many analyses were between 20-30 s in order to prevent damage to the slide.

Data reduction was conducted off-line using Iolite software. Base levels were determined through ^{43}Ca peak analysis making sure to avoid anomalous intensities but also including washout periods. Analytical drift was addressed by running a linear regression through average ^{43}Ca intensities in the NIST SRM610 runs before and after unknown analyses; reproducibility in was better than 5% for all elements analysed in NIST SRM610. Average concentrations of all elements were within error of published values (*Jochum et al.*, 2011) (Table SI-4, Supporting Data). REE values were normalized to chondrite (McDonough and Sun 1995) using Microsoft Excel, following methods outlined in *Rollinson* (1993).

LA-ICP-MS U-Pb calcite dating was conducted at the Geochronology & Tracers Facility, British Geological Survey (Nottingham, UK) using a New Wave Research 193UC excimer laser ablation system, coupled to a Nu Instruments Attom single-collector sector-field ICP-MS following the methods outlined by *Roberts and Walker* (2016). Samples were pre-ablated with a 150 µm spot for 30 pulses. Full ablation conditions comprise a 100 µm spot for 30 seconds, at 10 Hz and a fluence of ca. 8 J/cm^2. A gas blank of ca. 60 seconds is measured at the beginning of each run. Normalisation uses NIST614 for ^{207}Pb/^{206}Pb and WC-1 for ^{206}Pb/^{238}U, with data reduction and uncertainty propagation following *Roberts et al.* (2017) and the recommendations of (*Horstwood et al.*, 2016), and conducted using an in-house spreadsheet and the Nu Attolab Time Resolved Acquisition software. Spot analyses with low count rates (< 100 cps) or high uncertainties (>7.5% 1σ) are removed from age calculations. Age calculations and plotting were conducted using Isoplot 4.15 (*Ludwig*, 2003). Duff Brown Tank limestone was analysed during the session as a validation material; an age of 63.5±1.7 Ma (MSWD = 2.9) was obtained (Table SI-5, Supporting Data), which overlaps the published age of 64.04±0.67 Ma (*Hill et al.*, 2016).

4 Results

The location of analyses of all types in the vein samples are shown in Figures SI-1 and SI-2 (Supporting Information) and standard and sample geochemical data are given in Tables SI-3 to SI-6 (Supporting Information). Across the 5 samples analysed, δ^{13}C ranged from -1.90‰ to -9.87‰ but with the majority between -3 and -4‰ (Table 1 and Table SI-1, Supporting Data). There was no

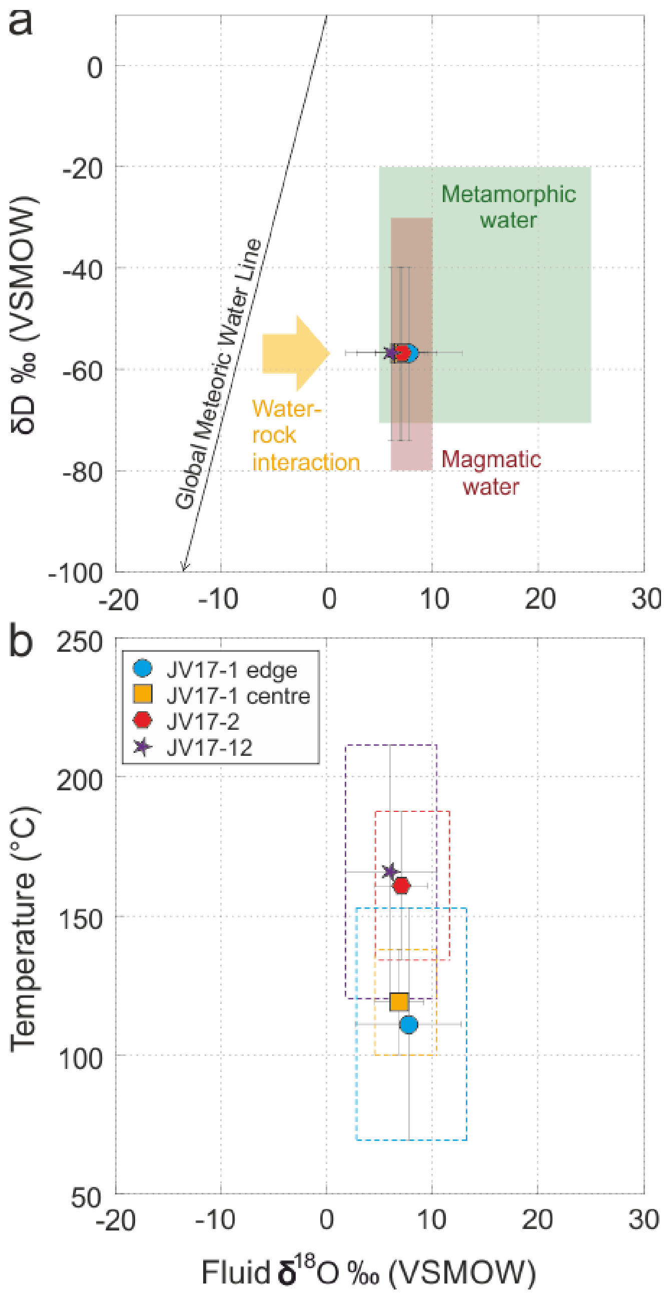

Figure 2 – Stable isotope data. **(a)** Fluid δD and calculated fluid δ^{18}O values using Friedman and O'Neil (1977) equation with the temperature and calcite δ^{18}O from clumped isotope analyses; δ^{18}O error bars are 1 standard error propagated from the clumped isotope analysis while δD error bars represent the range of δD values obtained during the analysis; Global Meteoric Water Line from Craig (1961); range of typical isotopic composition of metamorphic water (e.g. Taylor, 1974; Hoefs, 2015) and magmatic water (e.g. Hoefs, 2015). **(b)** temperature calculated using Bonifacie et al., (2017) Δ47-T calibration plotted against fluid δ^{18}O; temperature error bars are 95% confidence level while fluid δ^{18}O error bars are the conventional 1 standard error; dashed boxes constrain the 95% confidence level temperature error and the maximum range of fluid δ^{18}O calculated from the clumped isotope temperatures and the range of calcite δ^{18}O measured in the different samples. Blue circle = JV17-1 edge; orange square = JV17-1 centre; red hexagon = JV17-2; purple star = JV17-12.

clear correlation in $\delta^{13}C$ values and calcite crystal shape/vein texture or vein width at the point of analysis (Table SI-2, Supporting Data). Vein calcite $\delta^{18}O$ (V-PDB) values ranged from -1.36‰ to -13.21‰ (Table 1 and Table SI-1, Supporting Data). Narrower veins tended to have more depleted $\delta^{18}O$ values, although this did not hold true for all samples, and $\delta^{18}O$ varied by several permil in single veins (up to ~10.5‰ between two adjacent analyses in vein JV17-1) (Table 1 and Table SI-2, Supporting Data). A δD value of -56.8 was obtained from fluid inclusions in calcite chips from JV17-1 (Table 1, Figure 2). Four clumped isotope temperatures were determined from three of the samples. The edge of the large vein in sample JV17-1 yielded a temperature of 111±42°C while the centre of the same vein recorded 119±19°C. A temperature of 161±27°C was recorded from the centre of the large vein in JV17-2, and the set of sub-parallel linked veins in JV17-12 yielded a temperature of 166±46°C (Table 1, Figure 2b).

Fe concentrations were ~300-10000 ppm, with the majority <1000 ppm; Mn concentrations were ~700-12000 ppm. There was no clear correlation between Fe or Mn concentration and position across veins (i.e. edge to centre) and cathodoluminescence intensities were fairly uniform across all veins (Table 1, Figure SI-2, Supporting Information). Total Rare Earth Elements (ΣREE) values were ~1-1750 ppm (Table 1). In vein JV17-1, there was slight pattern of higher REE concentration at the vein edges than the core; however, this pattern was not present in the other wide (~30 mm diameter) vein (JV17-2) (Figure SI-2, Supporting Information). The other veins were too narrow (<1 mm in diameter) for an assessment of REE concentration across the vein. All analyses had higher light REE concentrations than heavy REEs. A number of analyses had flat normalised LREE-MREE patterns; La/Gd ratios were usually lower than Gd/Lu ratios (Table 1). Ce anomalies were negligible, with Ce/Ce* values of 0.7-1.2, representing slight negative to slight positive anomalies (Table 1). Eu anomalies were also mainly negligible, with slight negative (0.7) to slight positive (1.2) values; a small number of analyses recorded more positive anomalies (1.5-2.0) (Table 1, Table SI-4, Supporting Data).

One sample (JV17-2) yielded a calcite U-Pb age. The age of 318±30 Ma (MSWD = 1.4) was derived from regression of 89 spot analyses in that vein, with one analysis lying off the regression being rejected. This age includes propagation of the systematic uncertainties (Table 1, Figure 3).

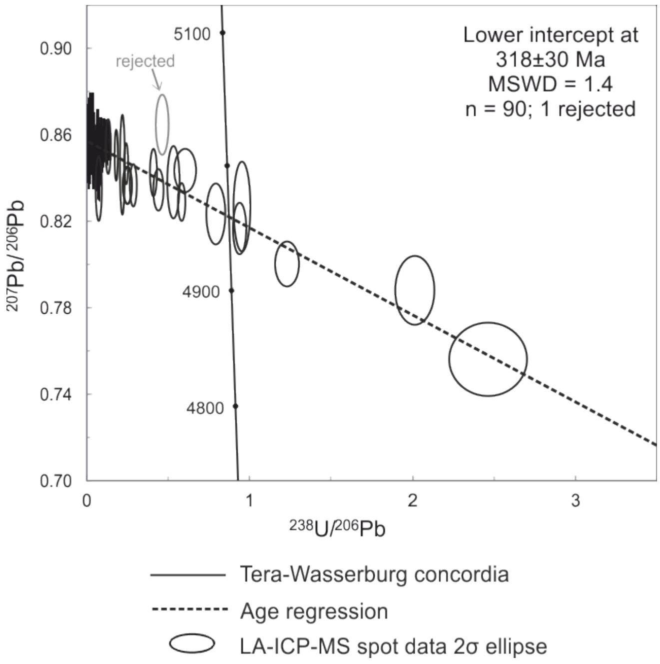

Figure 3 – Tera-Wasserburg concordia plot showing age regression through LA-ICP-MS analytical spots (blue ellipses; rejected spot in grey); precipitation age defined as the lower intercept age of 318±30 Ma (2σ).

5 Discussion

5.1 Stable Isotopes

Calcite which has resided in the subsurface at high temperatures (ca. >100°C) for a long period (ca. >100 Myr) is susceptible to solid-state bond reordering (*Passey and Henkes*, 2012; *Henkes et al.*, 2014; *Shenton et al.*, 2015; *Stolper and Eiler*, 2015; *Lloyd et al.*, 2018; *Hemingway and Henkes*, 2021). *Passey and Henkes* (2012) interpreted a two-stage bond reordering process of an initial phase of defect annealing followed by solid-state diffusion. *Stolper and Eiler* (2015) proposed different mechanisms: an initial rapid change of ~1-40°C at ambient temperatures of ~75-120°C sustained for ~100 Myr due to diffusion of isotopes through the crystal lattice; after a period of stability, a secondary stage of slow isotope exchange reactions between adjacent carbonate groups at >~150°C sustained for >~100 Myr which may bring the clumped isotope temperatures to the ambient temperature. Further experimental and theoretical work by *Hemingway and Henkes* (2021) showed that solid-state bond reordering arises from random-walk isotope diffusion through the mineral lattice. However, they found that the outcomes of solid-state bond reordering on clumped isotope temperatures vary little between these different proposed models, apart from at much higher temperatures where Δ_{47} re-equilibration is almost complete.

Given that the calcite U-Pb dating indicates that the veins are much older than ca. 100 Myr, and clumped isotope thermometry yields temperatures of ca. 100°C in all samples, thermal history reordering models (THRMs) were run to test for bond reordering (Table SI-6, Supporting Data). The THRM approach developed by *Shenton et al.* (2015) involves modelling temporal evolution in Δ_{47} based on kinetic parameters (e.g., activation energy, E_a and pre-exponential factor, K_o) derived from Arrhenius regressions of experimental data from

Table 1 – Summary data table; 'nd' denotes not enough water was recovered from these samples to make a measurement.

Sample	Description	δD (VSMOW,‰)	$\delta^{13}C$ (VPDB, ‰)	$\delta^{18}O_{cal}$ (VPDB, ‰)	$T_{\Delta 47}$ (°C)	$\delta^{18}O_{fluid}$ (VSMOW, ‰)	Mn (ppm)	Fe (ppm)	ΣREE (ppm)	La/Gd	Gd/Lu	Ce/Ce*	Eu/Eu*	U-Pb Age (Ma)
JV17-1	wide	-56.55	-1.90 to -5.21	-1.36 to -11.83	edge 111±42 centre 119±19	3.0 to 13.7 4.9 to 10.6	712-4230	373-846	4-1742	1.4-7.0	4.5-13.8	0.7-1.0	0.8-1.9	-
JV17-2	wide	nd	-3.46 to -4.55	-6.89 to -12.10	161±27	6.9 to 12.2	1996-6290	382-687	24-376	0.6-7.3	2.6-6.0	0.8-1.1	0.9-1.7	328±27
JV17-9	narrow	nd	-3.8 to -3.55	-8.25 to -9.51	-	-	7070-9380	719-1320	248-769	8.7-10.7	13.1-19.6	0.7-0.9	0.7-0.8	-
JV17-11	narrow	nd	-5.64 to -9.87	-10.77 to -12.89	-	-	3228-7001	447-5110	59-159	10.1-27.0	2.8-5.6	0.7-0.8	0.9-1.7	-
JV17-12	complex of connected sub-parallel narrow veins	nd	-3.04 to -3.35	-12.18 to -13.21	166±46	6.1 to 7.1	1780-5390	509-670	53-280	4.1-11.0	1.9-10.7	0.7-0.9	0.9-2.0	-

Passey and Henkes (2012). THRMs require knowledge or assumptions about the temperature history of the analysed sample. This temperature history is divided into a series of time steps with a specified ambient temperature (converted back to Δ_{47}) at each time step. The bond reordering reaction (reaction 13 in *Passey and Henkes*, 2012) is then used calculate the extent of clumped isotope reordering during each step. The 'new' Δ_{47} value at the end of each time step is treated as the 'initial' Δ_{47} value for the next step and the model is run iteratively from the time of initial calcite precipitation to the present day (*Shenton et al.*, 2015). Additionally, calcite of different origin (e.g. brachiopods vs spar calcite vs optical calcite) were found to have different reordering kinetics (activation energy and pre-exponential factor) during laboratory experiments (*Passey and Henkes*, 2012; *Henkes et al.*, 2014).

In addition to the activation energy and pre-exponential factor, the assumed initial precipitation temperature and age of precipitation are input to run the model. For sedimentary or biogenic calcite, an assumed surface temperature of ca. 25°C (or a more accurate one based on species in biogenic calcites) is used (*Henkes et al.*, 2013, 2014). For calcite veins this is challenging as one cannot assume an initial precipitation temperature. We assumed that the temperature reconstructed from clumped isotope analysis was the initial precipitation temperature and forward modelled using an ambient thermal history to determine if bond reordering had occurred.

THRMs were run for all samples using the burial history for the local area constructed from vitrinite reflectance data and an assumed geotherm of 30°C/km (*Marshall et al.*, 1994), along with the calcite precipitation ages derived in this study from LA-ICP-MS calcite U-Pb dating. Kinetic parameters for both optical and spar (labile and refractory) calcite from *Passey and Henkes* (2012) were used but the choice of kinetic parameters did not affect the model output. This is because the THRMs indicate that negligible (much less than analytical error) bond reordering took place in any of these samples (Figure 4).

Clumped isotope temperatures from the centre and edge of the large vein in sample JV17-1 are within error, suggesting that temperature remained relatively constant during calcite precipitation.

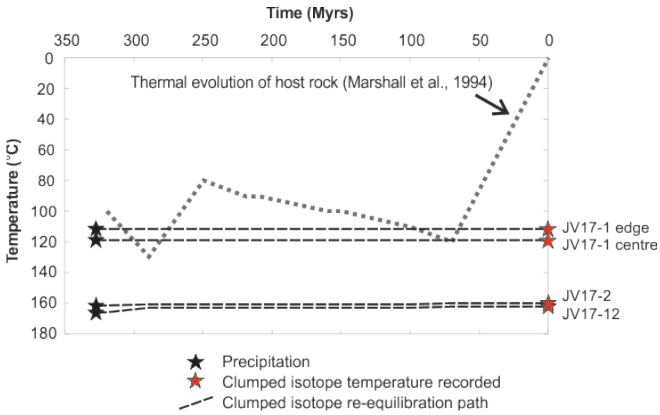

Figure 4 – Thermal history reordering models for vein samples where clumped isotope temperatures were obtained showing the modelled evolution of clumped isotope temperature (calculated using the equations in *Passey and Henkes* (2012) and the approach of *Shenton et al.* (2015)) and ambient temperature after vein precipitation (from *Marshall et al.*, 1994).

However, the temperatures from JV17-1 are ~50°C lower than in JV17-2 and JV17-12. The origin of this difference is unclear but may reflect an age difference – JV17-1 may be younger than JV17-2 and JV17-12 and records a cooling of the vein-forming fluid. Unfortunately, it was not possible to obtain an age from JV17-1 and so this cannot be proven. Calcite $\delta^{18}O$ (V-PDB) values varied by several permil within veins, suggesting that as well as some minor temperature variation within veins, slight variation in source fluid $\delta^{18}O$ and/or interaction with oxygen from the wall rocks of the veins resulted in variability in calcite $\delta^{18}O$. As the THRMs have shown that the clumped isotope temperatures do indeed represent the calcite precipitation temperature, the $\delta^{18}O$ of the parent fluids can be reconstructed.

In sample JV17-1, calculated fluid $\delta^{18}O$ (V-SMOW) values ranges from 3 to 14‰, but with the majority in the 7-9‰ range. Similarly for JV17-2, values are ~7-12‰, with most 7-9‰. In sample JV17-12, values are ~6-7‰ (Table 1, Figure 2). Values such as these represent fluids isotopically enriched relative to VSMOW and are typical of metamorphic waters, magmatic waters, or meteoric/marine waters which have undergone significant fluid-rock interaction (e.g. Sharp 2007). *Barker et al.* (2009) suggested that homogeneity of calcite $\delta^{18}O$ across veins may indicate the progressive reaction of fluids with host rock, with sufficient reaction occurring along discrete fluid flow pathways to fully equilibrate the fluids for these isotope systems. Samples JV17-9, JV17-11 and JV17-12 (narrow veins) display this homogeneity (<~2‰ variation), as does large vein JV17-2 apart from a single analysis at the very edge of the vein which is ~3‰ less depleted than the rest of the analyses from that vein (Figure SI-2, Supporting Information). Sample JV17-1, however, displays a wide range in calcite $\delta^{18}O$. Additionally, $\delta^{13}C$ values are all negative which suggest oxidised fluids (*Barker et al.*, 2006) which is more likely to be a surface water but is not conclusive. The δD values are also inconclusive and could represent metamorphic, magmatic or meteoric waters. Even when taking δD and $\delta^{18}O$ together, the samples fall within the field of typical magmatic and metamorphic waters or could represent meteoric water which has undergone significant water-rock interaction (e.g. *Taylor*, 1974; *Rollinson*, 1993; *Sharp*, 2017; *Hoefs*, 2015) (Figure 2b). Stable isotopes and reconstructed fluid $\delta^{18}O$ alone can therefore not distinguish fluid sources in this study.

5.2 Trace Elements

REE data for Old Red Sandstone (ORS) lavas closely related to the Lunan Bay rocks are given by *Thirlwall* (1982), and indicate that the host rocks are LREE enriched. The behaviour of REE during weathering and/ or fluid alteration of basalts and andesites varies strongly, depending on primary rock mineralogy, abundance of glass, temperature and fluid chemistry (e.g. *Wood et al.*, 1976; *Price et al.*, 1991), but it is likely that LREE and more mobile than heavy REE. Calcite additionally fractionates LREE over HREE during precipitation, leading to the negatively-sloping normalised REE patterns (e.g. *Bau et al.*, 1992; *Denniston et al.*, 1997; *Morad et al.*, 2010) as indicated by positive La/Gd and Gd/Lu ratios (Table 1). REE concentrations in the calcite veins in this study are higher than in typical freshwater/seawater (e.g. *Rollinson*, 1993; *Morad et al.*, 2010), suggesting metamorphic/magmatic fluids or freshwater/seawater which has undergone significant water-rock interaction. This agrees with the interpretation of the reconstructed fluid $\delta^{18}O$ values but still does not fingerprint a particular source fluid.

Conceptually, in narrow veins all the calcite might be expected to have higher REE concentrations given the lower calcite-wall rock ratio. This is not borne out by the total REEs but high La/Gd values – signifying strong fractionation of LREEs into the calcite – are found in narrow veins JV17-9 and JV17-11 (Table 1). JV17-9 in particular also shows the highest concentrations of Mn (Table 1). The volcanic wall rocks contain ~0.1 wt% MnO (Thirlwall 1982), again supporting the interpretation of significant fluid-rock interaction.

The veins generally showed no strongly positive Eu anomalies which suggests little interaction with Ca-rich bedrock, as Eu substitutes for Ca, predominantly in plagioclase (*Barker et al.*, 2006). The MVF is high in Ca (in clinopyroxene and plagioclase) and so extensive water-rock interaction would be expected to lead to positive Eu anomalies. This is generally not seen although some spots do have strongly positive Eu anomalies (up to 2.0); these do not appear to clearly correlate with position in the vein in relation to the wall rock or calcite petrography (Figure SI-2, Supporting Information). The Eu anomaly is therefore inconclusive regarding the origin of the fluid.

The Ce anomaly can be used as a redox proxy for fluids in veins, where a negative Ce anomaly indicates oxidising conditions (e.g. *Göb et al.*, 2013). No strongly negative (or positive) Ce anomalies were found in the veins in this study, indicating the fluid was not highly oxidised at the time of calcite precipitation. While well-oxidised surface waters have negative Ce anomalies, fluids which originate from the subsurface (magmatic/metamorphic fluids) or surface waters which have resided in the crust for some time and undergone water-rock interaction show no Ce anomaly (e.g. *Göb et al.*, 2013). The Ce anomaly is therefore in agreement with the stable isotope data, in that the fluid from which the veins precipitated from was either a magmatic/metamorphic fluid, or a meteoric/marine water which had undergone significant water-rock interaction. No correlation was found between calcite crystal microstructure and stable isotopes/trace elements (Figure SI-2, Supporting Information). This lack of correlation, and inability to fingerprint the source fluid, was also encountered by *Maskenskaya et al.* (2014) in a previous study.

5.3 Calcite Geochronology

Based on stable isotopes and trace elements, it has not been possible to distinguish the fluid source which formed the calcite veins between either a deep isotopically-enriched fluid (magmatic or metamorphic water) or a surface water which has undergone significant water-rock interaction. Based on the local geology, metamorphic waters can likely be ruled out as the fluid source as the nearest exposed metamorphic rocks are ~25 km away beyond the Highland Boundary Fault and the age of metamorphism (~470 Ma, *Viete et al.*, 2013) long predates the formation of the Devonian Montrose Volcanic Formation (MVF) host rocks to the calcite veins, thus the MVF was not yet formed during metamorphism.

Magmatic waters remain a viable fluid source as the host rocks are volcanic, and sporadic volcanic activity occurred through time in the Midland Valley Terrane (*Cameron and Stephenson*, 1985). Determining whether magmatic waters are a likely fluid source requires the age of calcite precipitation in the veins to be known, so that that age can then be compared to ages of volcanic/magmatic activity in the local area. If vein calcite precipitation occurred very soon after the formation of the MVF from residual waters from the volcanic activity, then the calcite should yield an age within error of the MVF crystallisation age. While the MVF has not been directly dated, the Rhynie Chert in the Lower Old Red Sandstone sequence with which it is correlated is dated at 411.5±1.3 Ma (*Parry et al.*, 2011). The MVF lavas are stratigraphically within the Arbuthnott-Garvock Group which spans ~420-410 Ma (*Hole et al.*, 2013). Given these constraints on the age of the host rock to the calcite veins, and the calcite precipitation age of 318±30 Ma, it is clear that the calcite did not form from a magmatic fluid associated with the formation of the host MVF. There is some Lower Carboniferous (potentially within uncertainty of the age from the Lunan Bay calcite veins) volcanic activity in the Midland Valley Terrane, but the nearest is located several tens of kilometres to the south around St Andrews (*Cameron and Stephenson*, 1985), and so it is unlikely that magmatic fluids associated with this volcanic activity were the source fluids for the calcite veins.

5.4 Importance of Calcite Geochronology in Fingerprinting Vein Fluid Sources

LA-ICP-MS U-Pb calcite dating has enabled us to rule out magmatic fluids as the source for calcite veins hosted in basaltic andesites when stable isotopes and trace elements were unable to do so. For the Lunan Bay calcite veins, the fluid source is suggested as a surface water which has undergone considerable fluid-rock interaction, leading to the enriched fluid $\delta^{18}O$ reconstructed from stable isotope analysis and clumped isotope thermometry. Palaeogeographic reconstructions indicate that the area was low-latitude coastal terrestrial lowland for much of the Carboniferous (*Cope et al.*, 1991), and we interpret that this surface water was likely meteoric water, rather than seawater/brine.

This case study from Lunan Bay highlights, along with previous studies from other locations (e.g. *Maskenskaya et al.*, 2014), the difficulty in fingerprinting fluid source from stable isotopes and/or trace elements. In this study, LA-ICP-MS U-Pb calcite geochronology helped eliminate potential fluid sources, enabling determination of the most likely fluid source for the analysed calcite veins. It is an additional proxy that should be used alongside stable isotopes and trace elements in studies where the fluid source of veins, or indeed any other geological feature where the parent fluid may have resided in the crust for a period of time such as fault precipitates (e.g. *Roberts and Walker*, 2016; *Parrish et al.*, 2018) or cements (e.g. *Mangenot et al.*, 2018b; *Pagel et al.*, 2018).

6 Conclusions

In this contribution we have shown that combining LA-ICP-MS U-Pb calcite dating with stable isotopes (including clumped isotope palaeothermometry) and trace element analysis increases the likelihood of determining the fluid source of veins. Calcite veins hosted in the Devonian Montrose Volcanic Formation at Lunan Bay in the Midland Valley Terrane of Central Scotland were used as a case study. δD values of fluid inclusions in the calcite, and parent fluid $\delta^{18}O$ values reconstructed from clumped isotope palaeothermometry, gave values which could represent a range of fluid sources: metamorphic or magmatic fluids, or surface waters which had undergone much fluid-rock interaction. Trace elements showed no distinctive patterns and shed no further light on fluid source. LA-ICP-MS U-Pb dating determined the vein calcite precipitation age – 318±30 Ma – which rules out metamorphic or magmatic fluid sources as no metamorphic or magmatic activity was occurring in the area at this time. The vein fluid source was therefore a surface water (meteoric based on paleogeographic reconstruction) which had undergone significant water-rock interaction. This study highlights the importance of combining the recently developed LA-ICP-MS U-Pb calcite geochronometer with stable isotopes and trace elements to help determine fluid sources of veins, and indeed any geological feature where calcite precipitated from a fluid which may have resided in the crust for a period of time (e.g. fault precipitates or cements).

Acknowledgements

Dr James Brenan and Dan MacDonald, Dalhousie University, are thanked for assistance using LA-ICP-MS; Alison McDonald is helped for assistance with the stable isotope analysis at SUERC. The reviewers Everton Bongiolo and John Craddock are thanked for their comments which improved the manuscript. Renata Schmitt is thanked for editorial handling. J. VanderWal received funding from Dalhousie University's Shell Educational Learning Fund (SELF) and the Society of Economic Geologists Canada Foundation (SEGCF) undergraduate research fund. Fieldwork was part-funded by Research Incentive Grant 70316 from the Carnegie Trust for the Universities of Scotland to J. M. MacDonald and J. W. Faithfull.

Author contributions

J. M. MacDonald: conceptualization; methodology; funding acquisition; supervision; writing (original draft); investigation; data curation; visualization. **J. VanderWal:** conceptualization; methodology; funding acquisition; writing (review and editing);

investigation; data curation; visualization. **N. M. W. Roberts:** methodology; writing (review and editing); investigation. **I. Z. Winkelstern:** methodology; writing (review and editing); investigation. **J. W. Faithfull:** conceptualization; supervision; writing (review and editing); investigation. **A. J. Boyce:** methodology; writing (review and editing); investigation.

Data availability

Figures SI-1 and SI-2 are included in the Supporting Information document. Tables SI-1 to SI-6 can be found in the Supporting Data associated with this publication.

Competing interests

The authors declare no competing interests.

Peer review

This publication was peer-reviewed by Everton Bongiolo and John Craddock. The full peer-review report can be found here: tektonika.online/index.php/home/article/view/2/71

Copyright notice

References

Armstrong, M., and I. B. Paterson (1970), *The Lower Old Red Sandstone of the Strathmore Region*, HM Stationery Office.

Barker, C. E., and R. H. Goldstein (1990), Fluid-inclusion technique for determining maximum temperature in calcite and its comparison to the vitrinite reflectance geothermometer, *Geology*, *18*(10), 1003–1006, doi: 10.1130/0091-7613(1990)018<1003:FITFDM>2.3.CO;2.

Barker, S. L. L., and S. F. Cox (2011), Oscillatory zoning and trace element incorporation in hydrothermal minerals: insights from calcite growth experiments, *Geofluids*, *11*(1), 48–56, doi: 10.1111/j.1468-8123.2010.00305.x.

Barker, S. L. L., S. F. Cox, S. M. Eggins, and M. K. Gagan (2006), Microchemical evidence for episodic growth of antitaxial veins during fracture-controlled fluid flow, *Earth and planetary science letters*, *250*(1), 331–344, doi: 10.1016/j.epsl.2006.07.051.

Barker, S. L. L., V. C. Bennett, S. F. Cox, M. D. Norman, and M. K. Gagan (2009), Sm–Nd, sr, C and O isotope systematics in hydrothermal calcite–fluorite veins: Implications for fluid–rock reaction and geochronology, *Chemical geology*, *268*(1), 58–66, doi: 10.1016/j.chemgeo.2009.07.009.

Bau, M., P. Moeller, and 4. 3 Organic Geochemistry, 4. 0 Chemistry and Material Cycles, Departments, GFZ Publication Database, Deutsches GeoForschungsZentrum (1992), Rare-earth element fractionation in metamorphogenic hydrothermal calcite, magnesite and siderite, *Mineralogy and Petrology*, *45*, 231–246.

Bergman, S. C., K. W. Huntington, and J. G. Crider (2013), Tracing paleofluid sources using clumped isotope thermometry of diagenetic cements along the moab fault, utah, *American journal of science*, *313*(5), 490–515, doi: 10.2475/05.2013.03.

Bluck, B. J. (2000), Old red sandstone basins and alluvial systems of midland scotland, *Geological Society, London, Special Publications*, *180*(1), 417–437, doi: 10.1144/GSL.SP.2000.180.01.22.

Bongiolo, E. M., C. Renac, A. S. Mexias, M. E. B. Gomes, L. H. Ronchi, and P. Patrier-Mas (2011), Evidence of ediacaran glaciation in southernmost brazil through magmatic to meteoric fluid circulation in the porphyry–epithermal Au–Cu deposits of lavras do sul, *Precambrian research*, *189*(3), 404–419, doi: 10.1016/j.precamres.2011.05.007.

Bonifacie, M., D. Calmels, J. M. Eiler, J. Horita, C. Chaduteau, C. Vasconcelos, P. Agrinier, A. Katz, B. H. Passey, J. M. Ferry, and Others (2017), Calibration of the dolomite clumped isotope thermometer from 25 to 350 c, and implications for a universal calibration for all (ca, mg, fe) CO3 carbonates, *Geochimica et cosmochimica acta*, *200*, 255–279.

Browne, M., R. Smith, and A. M. Aitken (2002), Stratigraphical framework for the devonian (old red sandstone) rocks of scotland south of a line from fort william to aberdeen, https://nora.nerc.ac.uk/id/eprint/3231/1/Devonian[1].pdf, accessed: 2024-1-15.

Cameron, I. B., and D. Stephenson (1985), *British regional geology: the Midland Valley of Scotland*, HM Stationery Office.

Coogan, L. A., R. R. Parrish, and N. M. W. Roberts (2016), Early hydrothermal carbon uptake by the upper oceanic crust: Insight from in situ U-Pb dating, *Geology*, *44*(2), 147–150, doi: 10.1130/G37212.1.

Cope, J. C. W., J. K. Ingham, P. F. Rawson, and Geological Society of London (1991), *Atlas of Palaeogeography and Lithofacies*, Geological Society Memoirs, Geological Society, Bath, England.

Coplen, T. B., W. A. Brand, M. Gehre, M. Gröning, H. A. J. Meijer, B. Toman, and R. M. Verkouteren (2006), New guidelines for δ13C measurements, *Analytical chemistry*, *78*(7), 2439–2441, doi: 10.1021/ac052027c.

Craddock, J. P., P. Nuriel, A. R. C. Kylander-Clark, B. R. Hacker, J. Luczaj, and R. Weinberger (2022), Long-term (7 ma) strain fluctuations within the dead sea transform system from high-resolution U-Pb dating of a calcite vein, *GSA Bulletin*, *134*(5-6), 1231–1246, doi: 10.1130/B36000.1.

Craig, H. (1961), Isotopic variations in meteoric waters, *Science*, *133*(3465), 1702–1703, doi: 10.1126/science.133.3465.1702.

Dennis, K. J., H. P. Affek, B. H. Passey, D. P. Schrag, and J. M. Eiler (2011), Defining an absolute reference frame for 'clumped' isotope studies of CO2, *Geochimica et cosmochimica acta*, *75*(22), 7117–7131, doi: 10.1016/j.gca.2011.09.025.

Dennis, P. F., D. J. Myhill, A. Marca, and R. Kirk (2019), Clumped isotope evidence for episodic, rapid flow of fluids in a mineralized fault system in the peak district, UK, *Journal of the Geological Society*, *176*(3), 447–461, doi: 10.1144/jgs2016-117.

Denniston, R. F., C. K. Shearer, G. D. Layne, and D. T. Vaniman (1997), SIMS analyses of minor and trace element distributions in fracture calcite from yucca mountain, nevada, USA, *Geochimica et cosmochimica acta*, *61*(9), 1803–1818, doi: 10.1016/S0016-7037(97)00049-5.

Drost, K., D. Chew, J. A. Petrus, F. Scholze, J. D. Woodhead, J. W. Schneider, and D. A. T. Harper (2018), An image mapping approach to U-Pb LA-ICP-MS carbonate dating and applications to direct dating of carbonate sedimentation, *Geochemistry, Geophysics, Geosystems*, *19*(12), 4631–4648, doi: 10.1029/2018gc007850.

Eiler, J. M. (2007), "clumped-isotope" geochemistry—the study of naturally-occurring, multiply-substituted isotopologues, *Earth and planetary science letters*, *262*(3), 309–327, doi: 10.1016/j.epsl.2007.08.020.

Epstein, S., R. Buchsbaum, H. Lowenstam, and H. C. Urey (1951), CARBONATE-WATER ISOTOPIC TEMPERATURE SCALE, *GSA Bulletin*, *62*(4), 417–426, doi: 10.1130/0016-7606(1951)62[417:CITS]2.0.CO;2.

Friedman, I. (1977), Compilation of stable isotope fractionation factors of geochemical interest, *Data of Geochemistry*, pp. KK1–KK12.

Friedman, I., J. O'neil, and G. Cebula (1982), Two new carbonate stable-isotope standards, *Geostandards newsletter*, *6*(1), 11–12, doi: 10.1111/j.1751-908x.1982.tb00340.x.

Gleeson, S. A., S. Roberts, A. E. Fallick, and A. J. Boyce (2008), Micro-Fourier transform infrared (FT-IR) and δD value investigation of hydrothermal vein quartz: Interpretation of fluid inclusion δD values in hydrothermal systems, *Geochimica et cosmochimica acta*, *72*(18), 4595–4606, doi: 10.1016/j.gca.2008.06.014.

Göb, S., A. Loges, N. Nolde, M. Bau, D. E. Jacob, and G. Markl (2013), Major and trace element compositions (including REE) of mineral, thermal, mine and surface waters in SW germany and implications for water–rock interaction, *Applied geochemistry: journal of the International Association of Geochemistry and Cosmochemistry*, *33*, 127–152, doi: 10.1016/j.apgeochem.2013.02.006.

Hemingway, J. D., and G. A. Henkes (2021), A disordered kinetic model for clumped isotope bond reordering in carbonates, *Earth and planetary science letters*, *566*, 116,962, doi: 10.1016/j.epsl.2021.116962.

Henkes, G. A., B. H. Passey, A. D. Wanamaker, E. L. Grossman, W. G. Ambrose, and M. L. Carroll (2013), Carbonate clumped isotope compositions of modern marine mollusk and brachiopod shells, *Geochimica et cosmochimica acta*, *106*, 307–325, doi: 10.1016/j.gca.2012.12.020.

Henkes, G. A., B. H. Passey, E. L. Grossman, B. J. Shenton, A. Pérez-Huerta, and T. E. Yancey (2014), Temperature limits for preservation of primary calcite clumped isotope paleotemperatures, *Geochimica et cosmochimica acta*, *139*, 362–382, doi: 10.1016/j.gca.2014.04.040.

Herlambang, A., and C. M. John (2021), Combining clumped isotope and trace element analysis to constrain potential kinetic effects in calcite, *Geochimica et cosmochimica acta*, *296*, 117–130, doi: 10.1016/j.gca.2020.12.024.

Hill, C. A., V. J. Polyak, Y. Asmerom, and P. P. Provencio (2016), Constraints on a late cretaceous uplift, denudation, and incision of the grand canyon region, southwestern colorado plateau, USA, from U-Pb dating of lacustrine limestone, *Tectonics*, *35*(4), 896–906, doi: 10.1002/2016tc004166.

Hoareau, G., N. Crognier, B. Lacroix, C. Aubourg, N. M. W. Roberts, N. Niemi, M. Branellec, N. Beaudoin, and I. Suárez Ruiz (2021), Combination of Δ47 and U-Pb dating in tectonic calcite veins unravel the last pulses related to the pyrenean shortening (spain), *Earth and planetary science letters*, *553*, 116,636, doi: 10.1016/j.epsl.2020.116636.

Hodson, K. R., J. G. Crider, and K. W. Huntington (2016), Temperature and composition of carbonate cements record early structural control on cementation in a nascent deformation band fault zone: Moab fault, utah, USA, *Tectonophysics*, *690*, 240–252, doi: 10.1016/j.tecto.2016.04.032.

Hoefs, J. (2015), *Stable Isotope Geochemistry*, Springer International Publishing, doi: 10.1007/978-3-030-77692-3.

Hole, M., D. Jolley, A. Hartley, S. Leleu, N. John, and M. Ball (2013), Lava–sediment interactions in an old red sandstone basin, NE scotland, *Journal of the Geological Society*, *170*(4), 641–655, doi: 10.1144/jgs2012-107.

Horstwood, M. S. A., J. Košler, G. Gehrels, S. E. Jackson, N. M. McLean, C. Paton, N. J. Pearson, K. Sircombe, P. Sylvester, P. Vermeesch, J. F. Bowring, D. J. Condon, and B. Schoene (2016), Community-derived standards for LA - ICP - MS U-(Th-)Pb geochronology – uncertainty propagation, age interpretation and data reporting, *Geostandards and Geoanalytical Research*, *40*(3), 311–332, doi: 10.1111/j.1751-908x.2016.00379.x.

Jochum, K. P., U. Weis, B. Stoll, D. Kuzmin, Q. Yang, I. Raczek, D. E. Jacob, A. Stracke, K. Birbaum, D. A. Frick, D. Günther, and J. Enzweiler (2011), Determination of reference values for NIST SRM 610–617 glasses following ISO guidelines, *Geostandards and Geoanalytical Research*, *35*(4), 397–429, doi: 10.1111/j.1751-908X.2011.00120.x.

Kalliomäki, H., T. Wagner, T. Fusswinkel, and D. Schultze (2019), Textural evolution and trace element chemistry of hydrothermal calcites from archean gold deposits in the hattu schist belt, eastern finland: Indicators of the ore-forming environment, *Ore Geology Reviews*, *112*, 103,006, doi: 10.1016/j.oregeorev.2019.103006.

Li, P., H. Zou, F. Hao, X. Yu, G. Wang, and J. M. Eiler (2020), Using clumped isotopes to determine the origin of the middle permian qixia formation dolostone, NW sichuan basin, china, *Marine and Petroleum Geology*, *122*, 104,660, doi: 10.1016/j.marpetgeo.2020.104660.

Li, Q., R. R. Parrish, M. S. A. Horstwood, and J. M. McArthur (2014), U–Pb dating of cements in mesozoic ammonites, *Chemical geology*, *376*, 76–83, doi: 10.1016/j.chemgeo.2014.03.020.

Lloyd, M. K., U. Ryb, and J. M. Eiler (2018), Experimental calibration of clumped isotope reordering in dolomite, *Geochimica et cosmochimica acta*, *242*, 1–20, doi: 10.1016/j.gca.2018.08.036.

Looser, N., H. Madritsch, M. Guillong, O. Laurent, S. Wohlwend, and S. M. Bernasconi (2021), Absolute age and temperature constraints on deformation along the basal décollement of the jura fold-and-thrust belt from carbonate U-Pb dating and clumped isotopes, *Tectonics*, *40*(3), doi: 10.1029/2020tc006439.

Lu, Y.-C., S.-R. Song, P.-L. Wang, C.-C. Wu, H.-S. Mii, J. MacDonald, C.-C. Shen, and C. M. John

(2017), Magmatic-like fluid source of the chingshui geothermal field, NE taiwan evidenced by carbonate clumped-isotope paleothermometry, *Journal of Asian Earth Sciences*, *149*, 124–133, doi: 10.1016/j.jseaes.2017.03.004.

Lu, Y.-C., S.-R. Song, S. Taguchi, P.-L. Wang, E.-C. Yeh, Y.-J. Lin, J. MacDonald, and C. M. John (2018), Evolution of hot fluids in the chingshui geothermal field inferred from crystal morphology and geochemical vein data, *Geothermics*, *74*, 305–318, doi: 10.1016/j.geothermics.2017.11.016.

Ludwig, K. R. (2003), User's manual for IsoPlot 3.0, *A Geochronological Toolkit for Microsoft Excel*, *71*.

MacDonald, J. M., J. W. Faithfull, N. M. W. Roberts, A. J. Davies, C. M. Holdsworth, M. Newton, S. Williamson, A. Boyce, and C. M. John (2019), Clumped-isotope palaeothermometry and LA-ICP-MS U–Pb dating of lava-pile hydrothermal calcite veins, *Contributions to mineralogy and petrology. Beitrage zur Mineralogie und Petrologie*, *174*(7), 63, doi: 10.1007/s00410-019-1599-x.

Mangenot, X., M. Gasparrini, A. Gerdes, M. Bonifacie, and V. Rouchon (2018a), An emerging thermochronometer for carbonate-bearing rocks: Δ47 /(U-Pb), *Geology*, *46*(12), 1067–1070, doi: 10.1130/G45196.1.

Mangenot, X., M. Gasparrini, V. Rouchon, and M. Bonifacie (2018b), Basin-scale thermal and fluid flow histories revealed by carbonate clumped isotopes (Δ_{47}) - middle jurassic carbonates of the paris basin depocentre, *Sedimentology*, *65*(1), 123–150, doi: 10.1111/sed.12427.

Marshall, J. E. A., P. D. W. Haughton, and S. J. Hillier (1994), Vitrinite reflectivity and the structure and burial history of the old red sandstone of the midland valley of scotland, *Journal of the Geological Society*, *151*(3), 425–438, doi: 10.1144/gsjgs.151.3.0425.

Maskenskaya, O. M., H. Drake, C. Broman, J. K. Hogmalm, G. Czuppon, and M. E. Åström (2014), Source and character of syntaxial hydrothermal calcite veins in paleoproterozoic crystalline rocks revealed by fine-scale investigations, *Geofluids*, *14*(4), 495–511, doi: 10.1111/gfl.12092.

Menzies, C. D., D. A. H. Teagle, D. Craw, S. C. Cox, A. J. Boyce, C. D. Barrie, and S. Roberts (2014), Incursion of meteoric waters into the ductile regime in an active orogen, *Earth and planetary science letters*, *399*, 1–13, doi: 10.1016/j.epsl.2014.04.046.

Morad, S., I. S. Al-Aasm, M. Sirat, and M. M. Sattar (2010), Vein calcite in cretaceous carbonate reservoirs of abu dhabi: Record of origin of fluids and diagenetic conditions, *Journal of Geochemical Exploration*, *106*(1), 156–170, doi: 10.1016/j.gexplo.2010.03.002.

Nuriel, P., R. Weinberger, A. R. C. Kylander-Clark, B. R. Hacker, and J. P. Craddock (2017), The onset of the dead sea transform based on calcite age-strain analyses, *Geology*, *45*(7), 587–590, doi: 10.1130/G38903.1.

Nuriel, P., J. Craddock, A. R. C. Kylander-Clark, I. Tonguç Uysal, V. Karabacak, R. K. Dirik, B. R. Hacker, and R. Weinberger (2019), Reactivation history of the north anatolian fault zone based on calcite age-strain analyses, *Geology*, *47*(5), 465–469, doi: 10.1130/G45727.1.

Pagel, M., M. Bonifacie, D. A. Schneider, C. Gautheron, B. Brigaud, D. Calmels, A. Cros, B. Saint-Bezar, P. Landrein, C. Sutcliffe, D. Davis, and C. Chaduteau (2018), Improving paleohydrological and diagenetic reconstructions in calcite veins and breccia of a sedimentary basin by combining Δ47 temperature, δ18Owater and U-Pb age, *Chemical geology*, *481*, 1–17, doi: 10.1016/j.chemgeo.2017.12.026.

Parrish, R. R., C. M. Parrish, and S. Lasalle (2018), Vein calcite dating reveals pyrenean orogen as cause of paleogene deformation in southern england, *Journal of the Geological Society*, *175*(3), 425–442, doi: 10.1144/jgs2017-107.

Parry, S. F., S. R. Noble, Q. G. Crowley, and C. H. Wellman (2011), A high-precision U–Pb age constraint on the rhynie chert Konservat-Lagerstätte: time scale and other implications, *Journal of the Geological Society*, *168*(4), 863–872, doi: 10.1144/0016-76492010-043.

Passey, B. H., and G. A. Henkes (2012), Carbonate clumped isotope bond reordering and geospeedometry, *Earth and planetary science letters*, *351-352*, 223–236, doi: 10.1016/j.epsl.2012.07.021.

Price, R. C., C. M. Gray, R. E. Wilson, F. A. Frey, and S. R. Taylor (1991), The effects of weathering on rare-earth element, Y and ba abundances in tertiary basalts from southeastern australia, *Chemical geology*, *93*(3), 245–265, doi: 10.1016/0009-2541(91)90117-A.

Purvis, K., P. Dennis, L. Holt, and A. Marca (2020), The origin of carbonate cements in the hildasay reservoir, cambo field, Faroe-Shetland basin; clumped isotopic analysis and implications for reservoir performance, *Marine and Petroleum Geology*, *122*, 104,641, doi: 10.1016/j.marpetgeo.2020.104641.

Ramsay, J. G., and M. I. Huber (1983), *The Techniques of modern structural geology. Volume 1: Strain analysis*, Academic Press.

Riegel, H., G. Casale, F. Mirabella, E. Hyland, and L. Talegalli (2022), Deep external fluid source along the gubbio normal fault (italy): Implications for slip along the altotiberina active Low-Angle normal fault system, *Frontiers of Earth Science in China*, *10*, doi: 10.3389/feart.2022.811339.

Ring, U., and A. Gerdes (2016), Kinematics of the Alpenrhein-Bodensee graben system in the central alps: Oligocene/Miocene transtension due to formation of the western alps arc, *Tectonics*, *35*(6), 1367–1391, doi: 10.1002/2015tc004085.

Roberts, N. M. W., and R. J. Walker (2016), U-Pb geochronology of calcite-mineralized faults: Absolute timing of rift-related fault events on the northeast atlantic margin, *Geology*, *44*(7), 531–534, doi: 10.1130/G37868.1.

Roberts, N. M. W., E. T. Rasbury, R. R. Parrish, C. J. Smith, M. S. A. Horstwood, and D. J. Condon (2017), A calcite reference material for LA-ICP-MS U-Pb geochronology, *Geochemistry, Geophysics, Geosystems*, *18*(7), 2807–2814, doi: 10.1002/2016GC006784.

Rollinson, H. R. (1993), *Using Geochemical Data*, 1st edition ed., Routledge, doi: 10.4324/9781315845548.

Schauble, E. A., P. Ghosh, and J. M. Eiler (2006), Preferential formation of 13C–18O bonds in carbonate minerals, estimated using first-principles lattice dynamics, *Geochimica et cosmochimica acta*, *70*(10), 2510–2529, doi: 10.1016/j.gca.2006.02.011.

Sharp, Z. (2017), *Principles of Stable Isotope Geochemistry, 2nd edition*, digitalrepository.unm.edu, doi: 10.25844/h9q1-0p82.

Shenton, B. J., E. L. Grossman, B. H. Passey, G. A. Henkes, T. P. Becker, J. C. Laya, A. Perez-Huerta, S. P. Becker, and M. Lawson (2015), Clumped isotope thermometry in deeply buried sedimentary carbonates: The effects of bond reordering and recrystallization, *GSA Bulletin*, *127*(7-8), 1036–1051, doi: 10.1130/B31169.1.

Simmons, S. F., and B. W. Christenson (1994), Origins of calcite in a boiling geothermal system, *American journal of physiology. Renal physiology*.

Staudigel, P. T., S. Murray, D. P. Dunham, T. D. Frank, C. R. Fielding, and P. K. Swart (2018), Cryogenic brines as diagenetic fluids: Reconstructing the diagenetic history of the victoria land basin using clumped isotopes, *Geochimica et cosmochimica acta*, *224*, 154–170, doi: 10.1016/j.gca.2018.01.002.

Stolper, D. A., and J. M. Eiler (2015), The kinetics of solid-state isotope-exchange reactions for clumped isotopes: A study of inorganic calcites and apatites from natural and experimental samples, *American journal of science*, *315*(5), 363–411, doi: 10.2475/05.2015.01.

Sturrock, C. P., E. J. Catlos, N. R. Miller, A. Akgun, A. Fall, R. I. Gabitov, I. O. Yilmaz, T. Larson, and K. N. Black (2017), Fluids along the north anatolian fault, niksar basin, north central turkey: Insight from stable isotopic and geochemical analysis of calcite veins, *Journal of Structural Geology*, *101*, 58–79, doi: 10.1016/j.jsg.2017.06.004.

Swennen, R., E. van der Voet, W. Wei, and P. Muchez (2021), Lower carboniferous fractured carbonates of the campine basin (NE-Belgium) as potential geothermal reservoir: Age and origin of open carbonate veins, *Geothermics*, *96*, 102,147, doi: 10.1016/j.geothermics.2021.102147.

Taylor, H. P. (1974), The application of oxygen and hydrogen isotope studies to problems of hydrothermal alteration and ore deposition, *Economic geology and the bulletin of the Society of Economic Geologists*, *69*(6), 843–883, doi: 10.2113/gsecongeo.69.6.843.

Thirlwall, M. F. (1981), Implications for caledonian plate tectonic models of chemical data from volcanic rocks of the british old red sandstone, *Journal of the Geological Society*, *138*(2), 123–138, doi: 10.1144/gsjgs.138.2.0123.

Thirlwall, M. F. (1982), Systematic variation in chemistry and Nd-Sr isotopes across a caledonian calc-alkaline volcanic arc: implications for source materials, *Earth and planetary science letters*, *58*(1), 27–50, doi: 10.1016/0012-821X(82)90101-7.

Thirlwall, M. F. (1983), Isotope geochemistry and origin of calc-alkaline lavas from a caledonian continental margin volcanic arc, *Journal of Volcanology and Geothermal Research*, *18*(1), 589–631, doi: 10.1016/0377-0273(83)90027-6.

Trewin, N. H. (2002), *The Geology of Scotland*, Geological Society of London.

Uysal, I. T., Y.-X. Feng, J.-X. Zhao, R. Bolhar, V. Işik, K. A. Baublys, A. Yago, and S. D. Golding (2011), Seismic cycles recorded in late quaternary calcite veins: Geochronological, geochemical and microstructural evidence, *Earth and planetary science letters*, *303*(1), 84–96, doi: 10.1016/j.epsl.2010.12.039.

Viete, D. R., G. J. H. Oliver, G. L. Fraser, M. A. Forster, and G. S. Lister (2013), Timing and heat sources for the barrovian metamorphism, scotland, *Lithos*, *177*, 148–163, doi: 10.1016/j.lithos.2013.06.009.

Wagner, T., A. J. Boyce, and J. Erzinger (2010), Fluid-rock interaction during formation of metamorphic quartz veins: A REE and stable isotope study from the rhenish massif, germany, *American Journal of*.

Weinberger, R., P. Nuriel, A. R. C. Kylander-Clark, and J. P. Craddock (2020), Temporal and spatial relations between large-scale fault systems: Evidence from the Sinai-Negev shear zone and the dead sea fault, *Earth-Science Reviews*, *211*, 103,377, doi: 10.1016/j.earscirev.2020.103377.

Wood, D. A., I. L. Gibson, and R. N. Thompson (1976), Elemental mobility during zeolite facies metamorphism of the tertiary basalts of eastern iceland, *Contributions to mineralogy and petrology. Beitrage zur Mineralogie und Petrologie*, *55*(3), 241–254, doi: 10.1007/bf00371335.